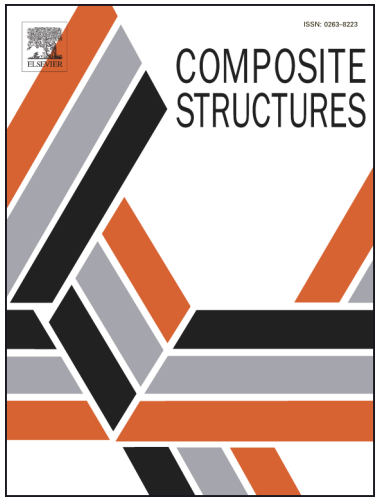

An Interval Updating Model for Composite Structures Optimization

Qinghe Shi, Xiaojun Wang, Ruixing Wang, Xiao Chen, Yujia Ma

PII: S0263-8223(18)32370-5
DOI: https://doi.org/10.1016/j.compstruct.2018.10.055
Reference: COST 10306

To appear in: *Composite Structures*

Received Date: 5 July 2018
Revised Date: 11 September 2018
Accepted Date: 19 October 2018

Please cite this article as: Shi, Q., Wang, X., Wang, R., Chen, X., Ma, Y., An Interval Updating Model for Composite Structures Optimization, *Composite Structures* (2018), doi: https://doi.org/10.1016/j.compstruct.2018.10.055

An Interval Updating Model for Composite Structures Optimization

Qinghe Shi[a] Xiaojun Wang[a,†] Ruixing Wang[b, c,†] Xiao Chen[a] Yujia Ma[a]

[a]*Institute of Solid Mechanics, Beihang University, Beijing 100083, China*

[b]*Key Laboratory for Mechanics in Fluid Solid Coupling Systems, Institute of Mechanics, Chinese Academy of Sciences, Beijing 100190, China*

[c]*School of Engineering Science, University of Chinese Academy of Science, Beijing 100049, China*

Abstract:

In practical engineering, the uncertainties commonly exist in the design process of composite structures due to the dispersion of composite materials. This paper proposes an uncertain optimization method based on interval model updating technique and non-probabilistic reliability (NPR) theory. A novel interval model updating method is firstly established by modifying the deterministic constraint condition parameters, which retains the quantification results of the material parameters and has a convinced updating model. In the design section, a new two-step optimization process for composite structures, which combines NPR method and progressive failure theory, is presented based on the updated simulation model. The traditional composite structural design method (safety factor based method) is also introduced to be compared. The NPR based optimization can optimize the nominal value and deviation of the structural response simultaneously, and will achieve a more significant weight reduction effect. A complete process including the uncertainty quantification, interval model updating, NPR based optimization and experimental verification for a composite stiffened plate under the compressive and shear load conditions were performed to verify the effectiveness of the proposed methodology.

Keywords: composite structural design; model updating; uncertainty; progressive failure analysis.

[†]Corresponding author: Xiaojun Wang. Email: xjwang@buaa.edu.cn; Tel: +86-010-82313658
[†]Corresponding author: Ruixing Wang. Email: wangruixing@imech.ac.cn; Tel: +86-010-82545792

1. Introduction

The composite materials with the advantages of high specific strength, high specific stiffness, fatigue resistance and corrosion resistance have been widely used in the design and manufacture of modern advanced structures. The composite provides a wider design space for the designers, and the optimization design of composite structures has been a hot topic by researchers [1, 2].

The composite structures have the excellent strength performance due to the post buckling loading capacity and anti-tearing properties. A lot of researches have been done to study the strength of the composite structures. The structural failure load is an important performance index to measure the performance of bearing capacity, therefore the structural failure criterion is the core issue. There are two different assumptions in the study of structural failure of laminate, namely, the first ply failure (FPF) criterion and the last ply failure (LPF) criterion. The FPF reckons that the laminate system is made of components in series and the failure of any layer in a single plate is regarded as failure of the system. This assumption is suitable for the problem with single loading path such as a pressure vessel with higher sealing requirement. Nevertheless, the FPF theory is too conservative in the most cases. The LPF reckons that the laminate system is made of parallel components. The remaining structure still has a certain bearing capacity after a single layer failure in the laminate structure. When all layers are in the failure, the structural system is defined as failure. The LPF is more close to the actual situation and attracts the attention of the composite designers. Lopez [3], Zhou [4], Qian [5] carried out a series of research of probabilistic system reliability based on the LPF criterion. However, the theory is hard to implement when the structure is complicated and all the failure paths are hard to determine entirely. Therefore, the scholars always launches research on the reliability by taking a single element as an object. Despite the FPF theory and LPF theory have high theoretical value, for practical engineering structures the failure load obtained by curve of the displacement to the load is an important experimental basis for measuring structural failure load. The corresponding computing process for the curve of the displacement to the load can be completed by the displacement loading mode and progressive failure analysis. The failure load is defined as the applied load at the point where the load is dropped with the increase of the displacement.

However, composites bring structural design challenges due to the uncertainty in the optimization. On the one hand, the dispersion induced in the manufacturing process will inevitably decrease the reliability of the optimization. On the other hand, the modelling error of the established FE model will lead to incorrect computing result.

There are two main methods to consider the dispersion of composites in the design procedure, namely the safety factor (SF) based method and reliability based method. SF is a magnification coefficient to cover the uncertain factors on the basis of production experience and design analysis. The SF is utilized as the envelope of the uncertainties, thus greatly simplifies the analysis process. A reasonable SF can better balance the relationship between the cost and the performance. It has been developed rapidly for composite structures in virtue of the briefness of the concept of SF, and some standards have been formed. In recent years, some scholars [6, 7] have proposed the method of obtaining the value of the SF based on the reliability theory to improve the efficiency of optimization. However, the SF based optimization method describes various uncertain factors conservatively, resulting in a waste of materials and the extreme redundancy of structural performance.

The reliability based design method which can not only optimize the nominal value but also the variance by refining the uncertainty in the process of structural design [8-11], has gradually drawn the attentions of scholars. The reliability analysis theory is to construct the reliability index through the uncertainty quantification for the uncertainty source in the design process, the uncertainty propagation analysis for the structural response and the reliability index computing by the intersection relationship between the uncertain response and its allowable value. Based on the probability reliability theory, the first-order second-moment (FOSM) [12], equivalent normalize [13] method (JC method) and the other methods [14-16] are developed to evaluate the reliability of laminated plates. Nevertheless, due to the condition of insufficient probability information, the optimization design based on the probability theory is difficult to apply in the actual engineering. By comparison, the non-probabilistic based reliability is more applicable to confront this situation. Recently, some scholars have concentrated on this issue and obtained some preliminary results. Wang [17] proposed non-probabilistic set-theoretic model for structural safety measure. Kang [18]

established a structural optimization model based on the uncertainty of convex model and proposed the optimization design method with the constraint condition of non-probabilistic reliability index. In general, the non probabilistic optimization design method is still in the developing stage, but the future development of it is wider due to the small dependence on the probability distribution information.

The model updating procedure is required to improve the precision of the FE model to decrease the uncertainty induced by the modelling error. It is noted that the model updating is a kind of inverse problem, which contains certain ill-conditioning in the solution process, caused by the incompatibility of the prediction model and its parameterization [19]. Nowadays, the regularization techniques [20] provide a solution by replacing the ill-posed problem with a well-conditioned one that has an approximate solution to the original problem. The regularization techniques are carried out to solve the ill-conditioning problem in a deterministic way, which has unstable results due to the selection of the samples. Fortunately, the uncertainty analysis method can quantify the influence of the uncertainties in the updating process and has derived applications [21]. The uncertain structural model updating methods can be divided into statistical based theory[22], fuzzy based method [23], interval theory based method [24, 25] and mixed models which combine statistical and interval (or fuzzy) method [26-29]. Among these methods, the interval methods have the advantage of low dependence on the sample numbers, which is suitable for situation of lack of data information. However, the existing interval methods deem that the initial intervals of the model parameters are updated to make the experimental responses be included by the FE model response. Although the operation is easy to be understood and always has fine results, it seldom exploits the intervals of model parameters, which are quantified by rigorous approach for the samples. Thus, this paper will propose a new interval model updating method to make the best of the intervals of the model parameters, and obtain a more reasonable FE model.

It should be noted that the composites have large number of design parameters including ply angles and ply thicknesses except for the geometric parameters, which will make the structural design a combined explosion problem. The coping strategy can be divided into two ideas, namely the effective optimization algorithm and the multistage strategy. The popular optimization

algorithms are permutation search (PS) algorithm [30] and particle swarm optimization (PSO) algorithm [31]. Although the global intelligent algorithm effectively improved the computational efficiency, the optimization process is still slow if the optimization strategy could not be simplified. Thus, a lot of scholars proposed hierarchical optimization strategy is always utilized to handle this [32, 33]. At the first level, the plate thicknesses are optimized to minimize the mass of the structure subject to strength and stiffness constraints. At the second level, a new modified particle swarm is used to determine laminate stacking sequences to search a better reserve factor for strength and stiffness. Despite the two-level optimization strategy may not lead to the global optimization in virtue of its rough decoupling mode, its convenient operation process and stable convergence can meet the composite structure design requirements. Additionally, some scholars studied the blended design scheme to obtain the manufacturable stacking sequence efficiently and provided repair strategy for dealing with continuity constraints [34]. Nevertheless, the above optimization have not taken the damage evolution and reliability analysis of the composite structures into account, which does not fully excavate the bearing potential of composite materials.

In view of the shortcomings of the uncertainty optimization study for the failure load of composite structures, this paper is aimed at developing a novel interval model updating based two-level optimization design method considering the inherent dispersion of materials for composite structures. The progressive failure analysis and the NPR theory are combined to construct the optimization model, and the two-level solution strategy is utilized to solve the optimization. This paper is organized in details as follows. In section 2, the model updating method under the condition of uncertainty is established. In section 3, the non-probabilistic failure load analysis method based on the progressive degradation theory is built up. In section 4, the optimization model based on SF index and NPR theory are constructed, respectively. To verify the proposed method, a composite stiffened plate under two load cases is carried out experimentally in section 5, in which the effectiveness between the SF based method and non-probability based method are compared. Finally the conclusions are summarized in section 6.

2. Structural model updating under the condition of uncertainty

In this part, the uncertainty quantification (UQ) is required to provide the quantified information of uncertain parameters for the interval updating procedure. In the following section, the UQ method this paper adopts is first introduced, then the interval model updating method is established.

2.1 Uncertainty quantification

Structural uncertainty analysis requires quantitative input data of uncertain sources. Generally, the UQ of uncertain parameters is based on experimental data, designing standard specifications, or past experience formula. Based on the classical probability theory, two kinds of criteria are given, namely, A basis value and B basis value. In recent years, a large number of researches have been carried out in view of the problem of normal distribution [35-37]. However, the sample information available in actual engineering structure design and service process is very limited. Thus, the non-probabilistic UQ analysis based on the finite samples becomes an important means in the field of uncertainty evaluation [38]. Among these methods, the grey mathematics method has the advantage of high efficiency and accuracy. The grey mathematics theory transforms the initial irregular data into a regular sequence by using data processing method. The dispersivity of the sample data are determined according to the dispersion of the regular sequence. Finally the information of uncertain parameters are gained [38, 39]. Compared with the traditional probability method and fuzzy method, the grey mathematics method requires smaller sample size, and has less subjective dependence. Therefore, the grey mathematics method is utilized to process the quantification for uncertain material parameters.

In engineering problems, any uncertain information can be used to obtain the interval estimation of real value. A set of measured data is listed as

$$\boldsymbol{X} = \{x(k), k = 1, 2, \ldots\ldots, n\}$$

The series of numbers can be arranged from small to large, and one can obtain

$$\boldsymbol{X}^{(0)} = \{x^{(0)}(k), k = 1, 2, \ldots\ldots, n\} \tag{1}$$

where $x^{(0)}(k) \le x^{(0)}(k+1), k = 1, 2, \cdots, n-1.$

The elements of $\boldsymbol{X}^{(0)}$ are added up in sequence, and a new sequence $\boldsymbol{X}^{(1)}$ can be obtained,

which can be expressed as

$$\begin{aligned}\boldsymbol{X}^{(1)} &= \left\{x^{(1)}(k), k=1,2,\ldots,n\right\} = \left\{x^{(1)}(1), x^{(1)}(2),\ldots, x^{(1)}(n)\right\} \\ &= \left\{x^{(0)}(1), x^{(0)}(1)+x^{(0)}(2),\ldots, x^{(0)}(1)+x^{(0)}(2)+\ldots+x^{(0)}(n)\right\}\end{aligned} \tag{2}$$

If one defines the following terms

$$\begin{cases}\Delta(k) = \dfrac{x^{(1)}(n)}{n}k - x^{(1)}(k) \\ \Delta_{\max} = \max(\Delta(1), \Delta(2), \ldots\ldots, \Delta(n)) \\ s = c\dfrac{\Delta_{\max}}{n}\end{cases} \tag{3}$$

where c is the constant grey coefficient, which is generally defined as 2.5; s is the estimated standard deviation of uncertainty based on grey evaluation. The above physical meaning of the estimation can be shown in Figure 1. The curved line represents the new sequence $\boldsymbol{X}^{(1)}$, which is called actual measurement process. When the dispersion is not considered, the value of each sample is defined as the arithmetic mean. The curved line is degenerated into the straight line, which is called the ideal measurement process. Taking normal distribution as an example, the interval bounds are reckoned as $[\bar{x}-3s, \bar{x}+3s]$, where $\bar{x} = \dfrac{1}{n}\sum_{i=1}^{n} x^{(0)}(i)$.

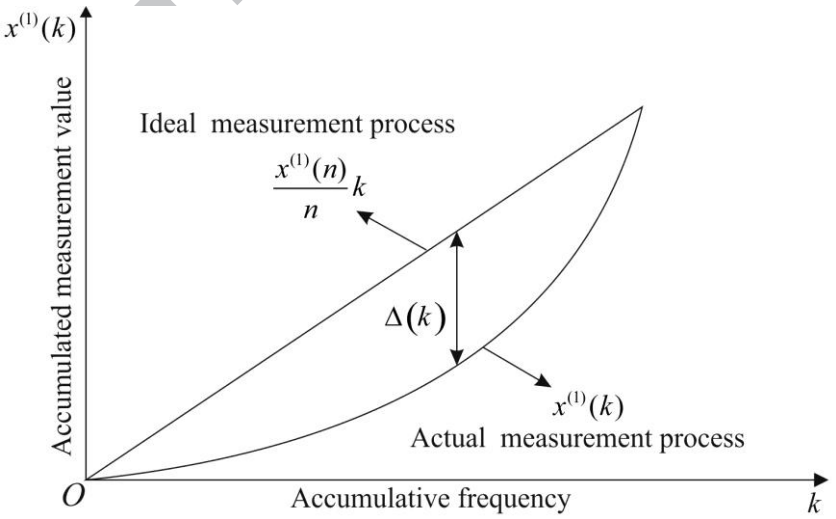

Figure 1 Schematic diagram of the grey system estimation method

The uncertainty quantification has two applications: one is to provide uncertainty input of the uncertainty analysis for the interval model updating and the optimization; the other is to determine the intervals of the experimental structural responses for the interval model updating.

2.2 Model updating based on the non-probabilistic interval theory

The difference between the simulated responses of FE model and actual structure originates in the following factors [40], the dispersion of material parameters, inaccuracy of boundary conditions and errors rooted in FEM. The dispersion of material comes from the defects in fiber and matrix and interfacial defects in the process of manufacturing. The boundary condition contains the connection stiffness between components, loading mode, sensor measurement errors and so forth. The simulation errors arise in the simplification of physical model and discretization error. The source of error considered in this paper are the uncertainty of material properties and boundary conditions, as the intrinsic error of simulation can be eliminated by the denser mesh for the FE model. In this paper, the boundary conditions are assumed to be deterministic variables due to the experiment equipment is unique.

The problems of mechanical analysis in this article can be expressed as the following form

$$\boldsymbol{y}^I = f\left(\boldsymbol{x}^I, \boldsymbol{P}\right) \tag{4}$$

where $\boldsymbol{y}^I = \{y_i^I\}$ is the interval structural response such as strain, stress, displacements, buckling load and failure load due to the uncertainty of material property; $\boldsymbol{x}^I = \{x_i^I\}$ is the interval of material parameter; $\boldsymbol{P} = \{P_i^I\}$ is the boundary condition to be updated. There are a number of samples of structural responses $\boldsymbol{y}$. The interval bounds of $\boldsymbol{x}$ are also known. The goal of the model updating is to determine the most possible value of $\boldsymbol{P}$.

In the probabilistic theory, the estimation of parameter $\boldsymbol{P}$ can be solved by moment estimation theory, maximum likelihood estimation and other estimation method. This paper will propose an interval model updating method to determine the boundary condition. The basic idea of the interval model updating method is to minimize the difference between the simulated interval bounds of structural responses and the experimental interval bounds of responses. The proposed method treat the interval material properties in the FE model and the experimental results the same important, in which the interval material properties of FE model are obtained from the mechanical testing. The structural model updating can be accomplished by optimization method.

$$\text{find} \quad \boldsymbol{P}$$

$$\min \quad \sum_{i=1}^{q} w_i \frac{\left|\underline{y_i^{exp}} - \underline{y_i^{sim}\left(\boldsymbol{P}, \boldsymbol{x}^I\right)}\right| + \left|\overline{y_i^{exp}} - \overline{y_i^{sim}\left(\boldsymbol{P}, \boldsymbol{x}^I\right)}\right|}{0.5*\left(\overline{y_i^{exp}} + \underline{y_i^{exp}}\right)} \tag{5}$$

where w_i is the weighting coefficient for the i-th structural response; $\underline{y_i^{exp}}, \overline{y_i^{exp}}$ are the interval bounds of i-th experimental structural response obtained from experimental samples; $\underline{y_i^{sim}\left(\boldsymbol{P}, \boldsymbol{x}^I\right)}, \overline{y_i^{sim}\left(\boldsymbol{P}, \boldsymbol{x}^I\right)}$ are the interval bounds of i-th simulated structural response on the basis of the uncertainties of material property. The objective function is to minimize the difference between the simulated interval bounds and the experimental bounds of structural responses. Taking the model updating based on single response as example, the interval model updating process can be illustrated in Figure 2. The blue lines are the interval bounds of the structural response, which vary as the boundary condition changes. The goal of the model updating is to make the simulated interval responses coincide with the experimental interval responses. The optimal solution of the model updating is P^*. When the structural responses become more, the optimal solution will be obtained by minimizing the summary of different responses multiplying the weighting coefficients.

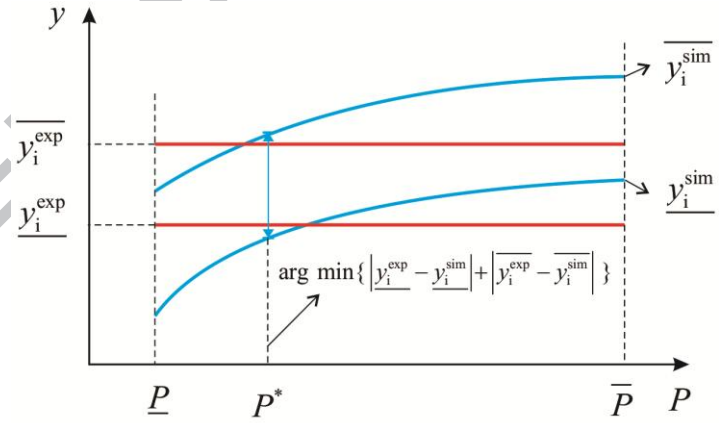

Figure 2 The interval bounds of simulated and experimental responses

3. The non-probabilistic failure load analysis based on the progressive degradation theory

In this paper, the optimization is for the reduction of weight and the improvement of structural carrying capacity. From the point of view of this paper, the reasonable calculation method for the failure should be the progressive failure analysis combined with the displacement-load curve. Considering the uncertainties in the material properties, this paper applies the non-probabilistic

theory into the solution of structural carrying capacity.

3.1. Failure load computing procedure based on the progressive degradation analysis

The structural failure analysis is based on the procedure of step loading and progressive degradation for materials. The structural failure is first initiated at local stress concentration, where the stress reaches the failure criterion, then the relative local stiffness decreases. The common failure criteria used for judging failure of material are Hashin criterion[41], Puck criterion[42], Chang criterion[43], LaRC04 criterion[44] and so on. The elastic parameters of the elements that satisfy the failure criterion will drop to small values. When a certain amount of elements on the cross section of the load-transferred path are failed, the constraint force will decrease as the displacement increases, namely the structural failure. The procedure of computing failure load is shown in Figure 3. The improved quadratic Hashin criterion [45] and the stiffness reduction scheme are given, respectively.

Longitudinal (one direction) tension failure $\left(\sigma_1>0\right)$

$$\left(\frac{\sigma_1}{X_t}\right)^2+\alpha\left(\frac{\tau_{12}}{S_{12}}\right)^2\geq 1 \tag{6}$$

Longitudinal (one direction) compression failure $\left(\sigma_1<0\right)$

$$\left(\frac{\sigma_1}{X_c}\right)^2\geq 1 \tag{7}$$

Transverse (two directions) tension failure $\left(\sigma_2>0\right)$

$$\left(\frac{\sigma_2}{Y_t}\right)^2+\alpha\left(\frac{\tau_{12}}{S_{12}}\right)^2\geq 1 \tag{8}$$

Transverse (two directions) compression failure $\left(\sigma_2<0\right)$

$$\left(\frac{\sigma_2}{Y_c}\right)^2\geq 1 \tag{9}$$

In-plane shearing failure:

$$\left(\frac{\tau_{12}}{S_{12}}\right)^2\geq 1 \tag{10}$$

where $\sigma_1, \sigma_2, \tau_{12}$ are the fiber direction stress, transverse stress and in-plane shear stress, respectively; $X_t, X_c, Y_t, Y_c, S_{12}$ are the longitudinal direction tensile strength, fiber direction compressive strength, transverse direction tensile strength, transverse direction compressive strength and in-plane shear strength, respectively; α is the contribution of the shear stress to the longitudinal and transverse tensile initiation.

When the above dimension failure criteria are satisfied, the material properties of the damage unit will be weakened. In different failure modes, elastic parameters can be degraded based on different rules [46, 47]. In this paper, the following material degeneration is adopted to characterize the damage of the laminate.

1) When the longitudinal tension failure happens, let E_1 be $0.07E_1$;
2) When the longitudinal compression failure happens, let E_1 be $0.14E_1$;
3) When the transverse tension failure happens, let E_2 be $0.07E_2$;
4) When the transverse compression failure happens, let E_2 be $0.14E_2$;
5) When the shearing failure happens, let E_{12} be $0.4E_{12}$.

The procedure of the progressive failure method is as follows, and the flowchart is shown in Figure 3. The calculation steps are as follows.

Step 1: initialize the FEM model, where the material parameters are in undamaged state;

Step 2: start the displacement loading;

Step 3: static analysis for the structure and extract the constraint force of the loading point;

Step 4: if the constraint force decline, output the failure load and finish the procedure, else extract the stress of the structure and proceed the next step;

Step 5: if the elemental stress tensor satisfies the failure criterion, reduce the elemental elastic moduli, else increase the displacement load and go to Step 3.

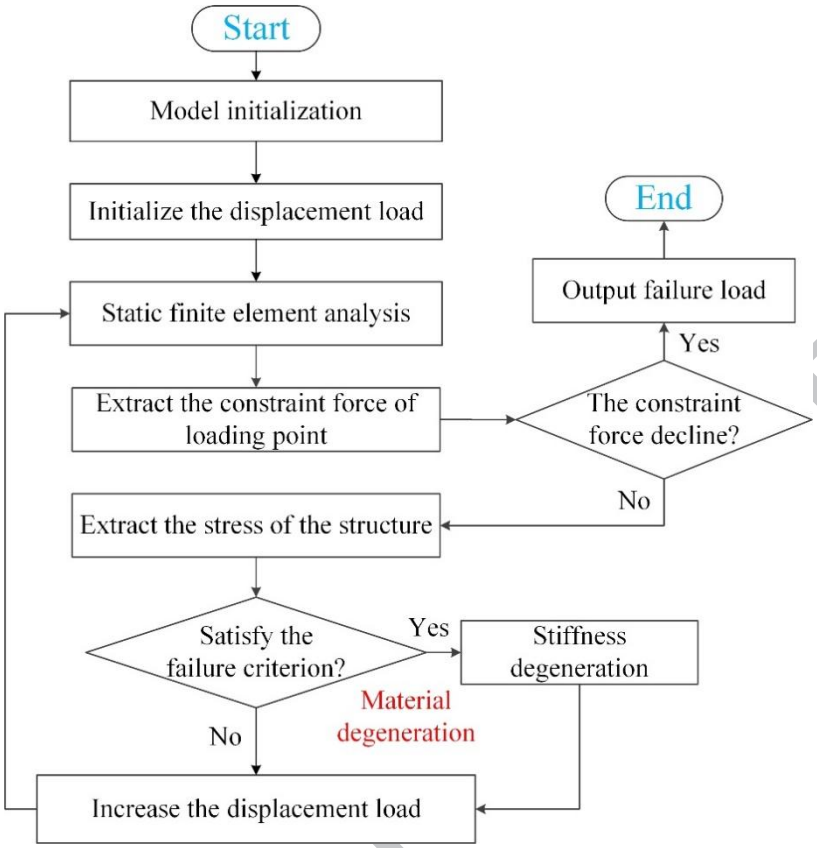

Figure 3 The flowchart of computing failure load

3.2. Non-probability reliability (NPR) analysis of failure load for composite

In this paper, the failure load analysis of composite structure is taken as a black box, in which the input is material parameter information and output is the interval of failure load.

The structural responses $\boldsymbol{y}^I$ are uncertain due to the dispersion of material parameters $\boldsymbol{x}^I$. The method of calculating the interval of structural responses can be divided into vertex method [48], series expansion method [49] and collocation method [50] according to the relationship between input uncertain parameters and structural responses.

The structure performance is usually marked by the limit state function established by the structural response and the allowable value. The stress–strength interference model [51] is introduced to define the NPR. Herein, for the convenience of description, S is short for the structural carrying capacity, and R is short for the allowable structural carrying capacity. S represents y_i that is shown in Eq.(4). The S and R are taken as the basic interval variables to illustrate the process of NPR solution.

$$S \in S^I = \left[\underline{S}, \overline{S}\right], \qquad R \in R^I = \left[\underline{R}, \overline{R}\right] \tag{11}$$

where I means the interval number; '¯' denotes the upper bound of the interval number; and '_' denotes the lower bounds of the interval number.

The structural limit state function is taken as

$$M\left(R,S\right) = R - S \tag{12}$$

where R and S space is divided into safety domains and failure domain by (12), and the dividing line is the failure plane as $M\left(R,S\right) = R - S = 0$. The interval variables of the corresponding force and strength are standardized as

$$\delta_S = \left(S - S^c\right)/S^r, \quad \delta_R = \left(R - R^c\right)/R^r \tag{13}$$

where $S^c = \left(\overline{S} + \underline{S}\right)/2, R^c = \left(\overline{R} + \underline{R}\right)/2, S^r = \left(\overline{S} - \underline{S}\right)/2, R^r = \left(\overline{R} - \underline{R}\right)/2$. The stress interval and the strength interval are interfered when the structure is likely to be dangerous, as shown in Figure 4 a). Although the central value of S is less than the central value of R, it cannot absolutely guaranteed that S is always less than R in any case. That is, the possibility that S is greater than R is positive, and is expressed as

$$\eta\left(M\left(\delta_R, \delta_S\right) < 0\right) > 0 \tag{14}$$

Similarly, the interference relationship between stress and strength in the one-dimensional axis can be converted to the interference relationship in two-dimensional normalized interval variable space, as shown in Figure 4 b). The possibility of failure can be defined as the ratio of the area of the failure domain to the total area of the basic variable.

$$F_{set} = \eta\left(M\left(\delta_R, \delta_S\right) < 0\right) = \frac{S_{failure}}{S_{total}} \tag{15}$$

Similarly, the reliability can be defined as the ratio of the area of the safety domain to the total area of the basic variable.

$$R_{set} = \eta\left(M\left(\delta_R, \delta_S\right) > 0\right) = 1 - \frac{S_{failure}}{S_{total}} \tag{16}$$

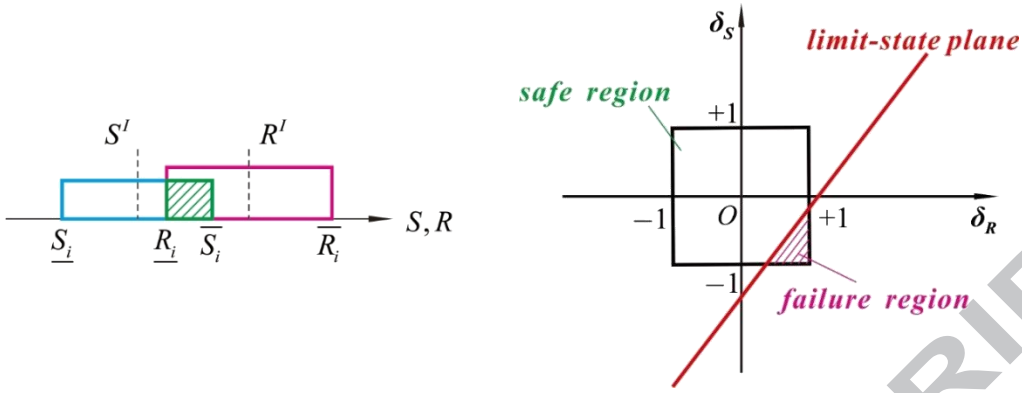

a) 1D R-S interference b) 2D R-S interference

Figure 4 Non-probabilistic R-S interference

4. The optimization approach for the improvement of the structural carrying capacity

To compare the optimization effect of the traditional method (SF based method) and the non-probability based method, the SF based method is firstly illustrated, and the non-probability based method is then presented. In the both methods, the two-level optimization strategy is adopted to decouple the design variables, namely the ply thickness and the angle.

4.1. Two-level optimization approach based on SF

In the SF based optimization method, the first step is to optimize the thicknesses or the numbers of layers with different angles when the lamina has a specific thickness. The second step is to optimize the stacking sequence of the laminates based on the first optimization results. The optimization model of the first step is shown as follows.

$$\begin{aligned} &\min \quad W \\ &\text{find} \quad t_{\theta_1}, t_{\theta_2}, \cdots \left(n_{\theta_1}, n_{\theta_2}, \cdots \right) \\ &\text{s.t.} \quad F_1 \geq n \times \left[F_1 \right], F_2 \geq n \times \left[F_2 \right], \cdots \end{aligned} \tag{17}$$

where W is the total mass of the structure; $t_{\theta_i}\left(n_{\theta_i}\right)$ is the thickness or the number of super layers with angle θ_i; F_j are the failure load of the *j*th load condition, which is calculated by the progressive failure analysis; $\left[F_j \right]$ are the critical failure load of the *j*th load condition. The objective is to minimize the weight of the structure. The constraint condition is that the failure loads satisfy the allowable values.

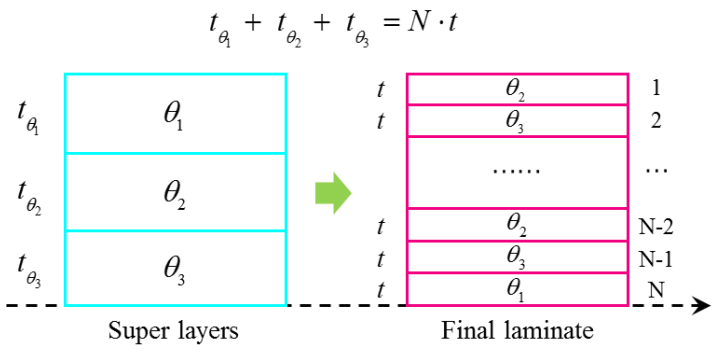

Figure 5 The super layers and final laminates

After the thicknesses of all super layers have been optimized in the first step, the stacking sequence optimization of the laminate is processed in the second step. The transformation from the super layers in the first step to the final laminates in the second step is illustrated in Figure 5. The optimization model of the second step is shown as follows.

$$\begin{aligned} \max \quad & F_1, F_2, \cdots \\ \text{find} \quad & \{\theta_u\}, (u = 0^\circ, 45^\circ, \cdots) \\ \text{s.t.} \quad & g_{j^*}(t) \le 0, \quad j^* = 1, 2, \cdots \\ & F_1 \ge n \times [F_1], \quad F_2 \ge n \times [F_2], \cdots \end{aligned} \tag{18}$$

where $\{\theta_u\}$ is the stacking sequence scheme; $g_{j^*}(t) \le 0$ is the processing constraints to be met in the layer scheme. The objective is to maximize the failure loads in different load cases. The constraint conditions are the manufacturing constraints and the failure loads are not less than the allowable values.

4.2. Two-level optimization approach based on NPR theory

Similarly to the SF based two-level optimization approach, the NPR based method is processed by the super layer optimization and the stacking sequence optimization except the failure load is replaced by the NPR index. The optimization model of the first step is shown as follows.

$$\begin{aligned} \min \quad & W \\ \text{find} \quad & t_{\theta_1}, t_{\theta_2}, \cdots \left(n_{\theta_1}, n_{\theta_2}, \cdots\right) \\ \text{s.t.} \quad & R\left(F_1^I\left(\boldsymbol{E}^I, \boldsymbol{X}^I\right) - [F_1]\right) \ge [R_{SF}^1] \\ & R\left(F_2^I\left(\boldsymbol{E}^I, \boldsymbol{X}^I\right) - [F_2]\right) \ge [R_{SF}^2] \\ & \cdots \end{aligned} \tag{19}$$

where $F_j^I\left(\boldsymbol{E}^I,\boldsymbol{X}^I\right)$, caused by the dispersion of strength parameters and elastic parameters, expresses the interval of the failure load of the *j*-th load condition, which is computed by progressive failure analysis and the interval mathematic theory. $R\left(F_j^I\left(\boldsymbol{E}^I,\boldsymbol{X}^I\right)-\left[F_j\right]\right)$ expresses the NPR of the failure load of the *j*-th load condition by the non-probabilistic set reliability theory. $\left[R_{SF}^1\right]$ expresses the NPR index of the *j*-th load condition of the optimization scheme based on SF method. Herein, $\boldsymbol{E}^I,\boldsymbol{X}^I$ represent $\boldsymbol{x}^{\mathrm{I}}$ in Eq.(4), and $F_j^I\left(\boldsymbol{E}^I,\boldsymbol{X}^I\right)$ expresses y_i^I in Eq.(4). In this step, the thicknesses of the laminate is optimized under the premise of the laminate has the reliability not worse than it based on the SF method.

After the thicknesses of the super layers have been optimized by the optimization model in (19), the stacking sequences can be optimized to raise the lower bounds of the failure load in different load conditions. The optimization model of the second step is shown as follows.

$$\begin{aligned}
&\max \quad \underline{F_1},\underline{F_2},\cdots \\
&\text{find} \quad \theta_u,(u=0^{\mathrm{o}},45^{\mathrm{o}},\cdots) \\
&\text{s.t.} \quad R\left(F_1^I\left(\boldsymbol{E}^I,\boldsymbol{X}^I\right)-\left[F_1\right]\right)\geq\left[R_{SF}^1\right] \\
&\qquad R\left(F_2^I\left(\boldsymbol{E}^I,\boldsymbol{X}^I\right)-\left[F_2\right]\right)\geq\left[R_{SF}^2\right] \\
&\qquad g_{j^*}(t)\leq 0,\quad j^*=1,2,\cdots
\end{aligned} \tag{20}$$

where $\underline{F_j}$ is the lower bound of the failure load of the *j*-th load condition.

Through the two-step NPR based optimization, the optimization scheme will be obtained with better bearing capacity. The flowchart of the whole procedure of this paper is illustrated in Figure 6. The whole process of the proposed method can be divided into 4 parts as model updating for the FEM model, optimization based on the SF, reliability analysis for the SF based optimization scheme and optimization based on non-probabilistic reliability. In every part, the progressive degradation analysis for the solution of failure load is involved.

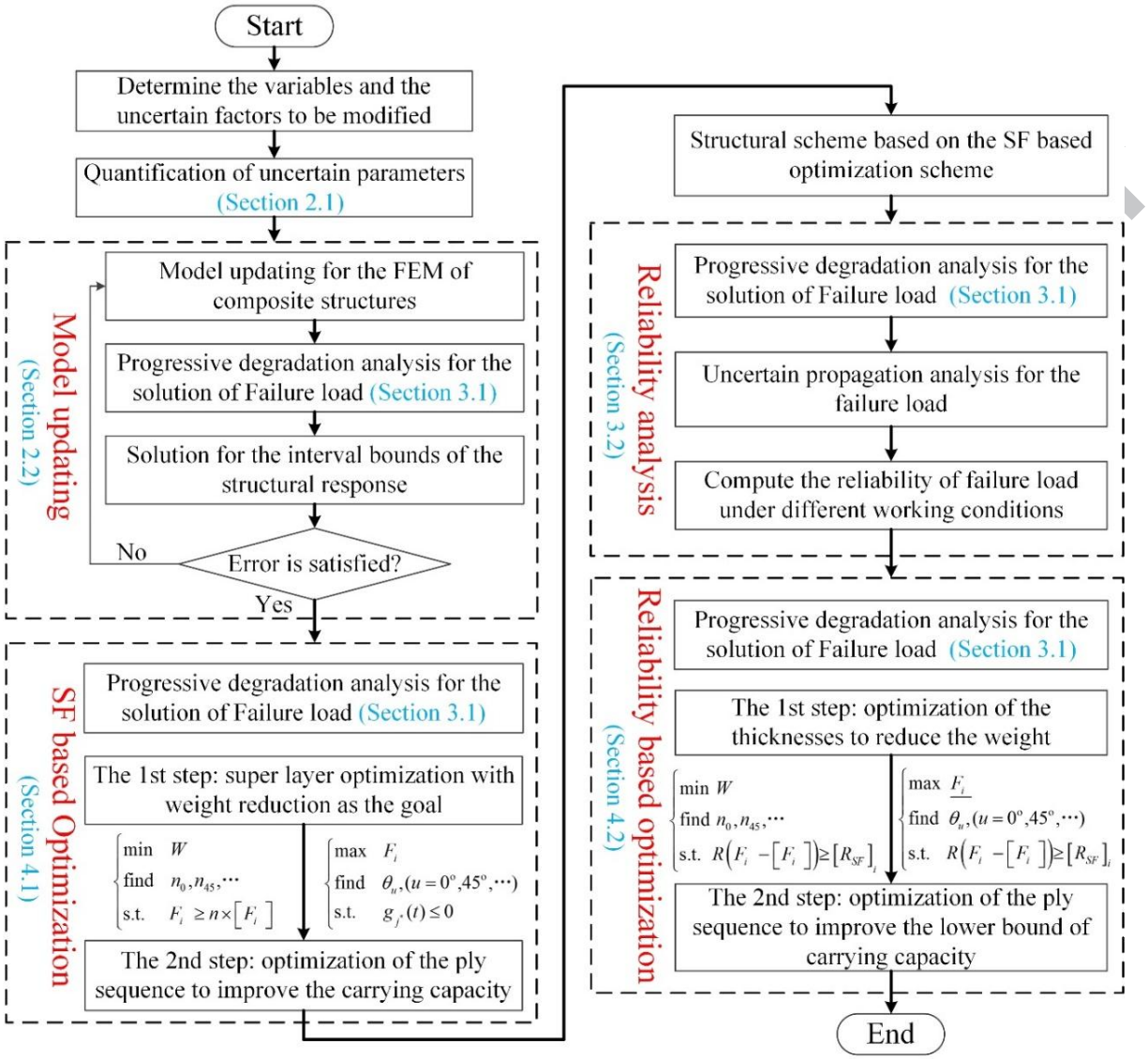

Figure 6 Flowchart of the optimization process

5. Experimental study

To verify the effectiveness of the proposed methodology, an experimental work of stiffened plates under two load cases as compressive and shear loads were processed. The typical stiffened plate of the optimization problem is selected from a kind of aircraft. All the composite components are made of T300/901. The T300/901 carbon/epoxy composite laminate is made of bidirectional carbon-fiber-impregnated materials (woven fabric composite material), and the single layer is 0.22 mm thickness. The FE models were updated firstly by the experimental results of the original layer scheme. Then the optimization based on the SF, reliability analysis for the SF based optimization

scheme and optimization based on non-probabilistic reliability were processed step by step. At last, the optimal layer scheme was verified experimentally.

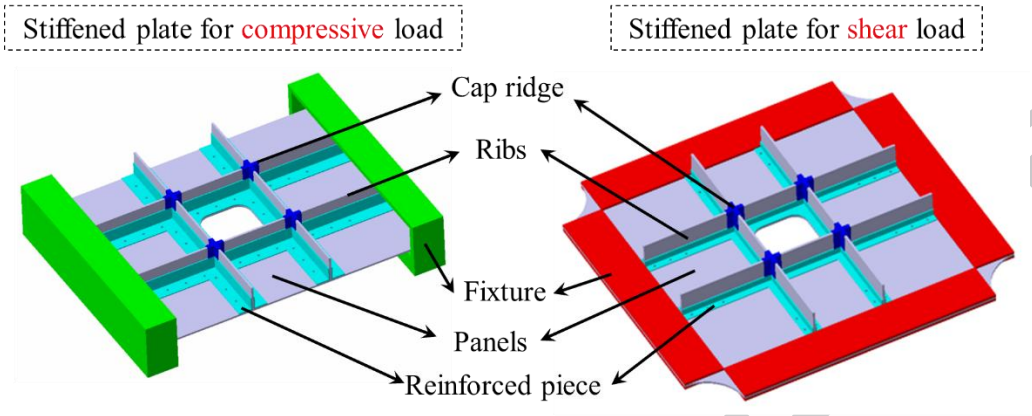

Figure 7 The CAD model of the stiffened plate for the compressive load and shear load

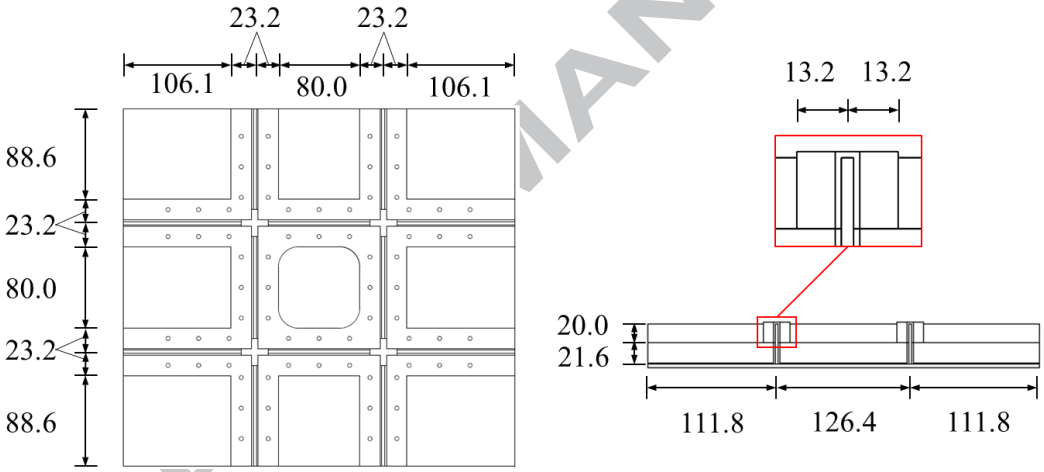

Figure 8 The dimension of the stiffened plate(mm)

The CAD models of the stiffened plate for the compressive load and shear load are shown in Figure 7. The stiffened plates contain panels, reinforced piece, ribs, cap ridge and fixture. The panels are the principle bearing parts, but have poor stability. The ribs are arranged to increase their stability and the reinforced piece, cap ridges are utilized to link the panels and the ribs. The two structures are basically the same except that the fixture are different due to the diverse load cases. The fixture parts are made of aluminum alloy and the other parts are made of fabric composites. The dimension of the stiffened plate are shown in Figure 8. In the initial scheme, the stacking sequence is $[45^{o}/0_{2}^{o}/45^{o}/0^{o}/\overline{45^{o}}]_{s}$ for all the composite parts. In view of the CAD model, the FEM model is established as shown in Figure 9.

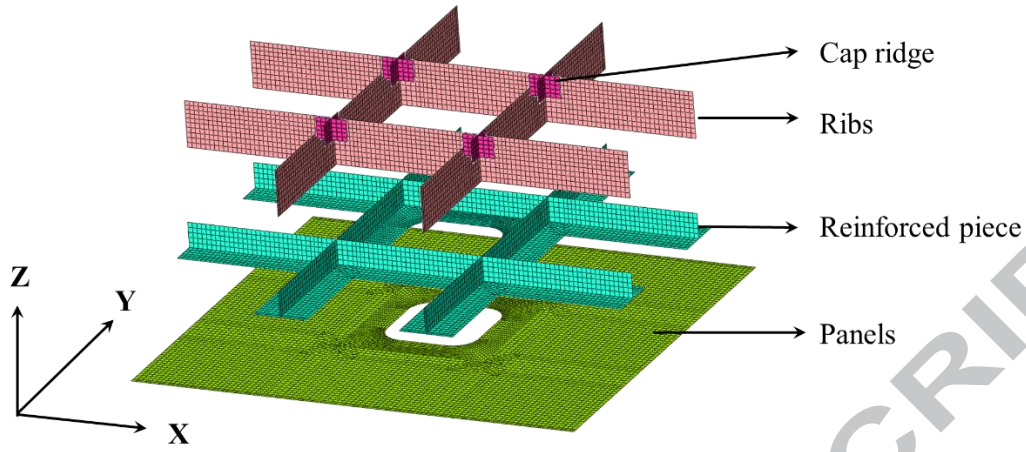

Figure 9 the FEM model of the stiffened plate

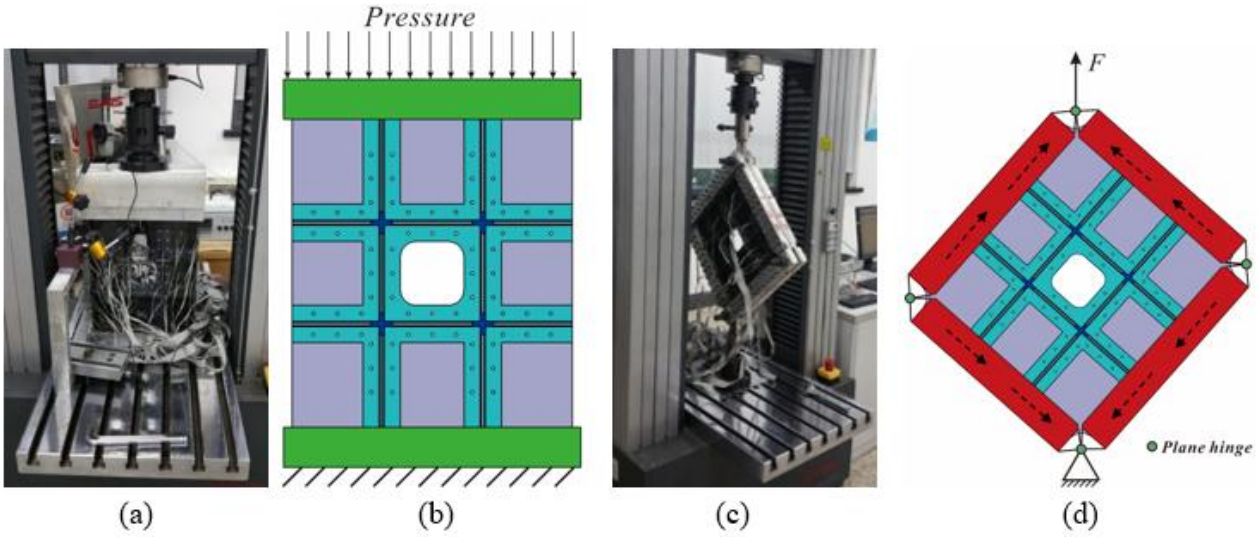

Figure 10 The experimental setup and loading sketch: (a) experimental setup of CLC; (b) loading sketch of CLC; (c) experimental setup of SLC (d) loading sketch of SLC.

The experimental setup and loading sketch of compressive loading condition (CLC) and shear loading condition (SLC) are shown in Figure 10. In the loading sketch of SLC, the tensile force is transformed on the fixtures through the plane hinge, which makes that the structure is under shear load. The FE models were modified on the basis of the experimental data before they were used to process the optimization.

In this experimental work, each test piece was tested including elastic state and limit state. The test of elastic state is loaded from 0 to 20kN with 2kN increments. The tests of limit state were loaded from 0 to 80kN by taking 5kN as loading step, and from 80kN until it were destroyed taking

0.5kN as loading step. There are 8 test samples as 4 specimens for the compressive test and 4 specimens for the shear test.

5.1. Model updating for the FE models in small sample situation

The interval boundaries of elastic parameters and strength parameters are listed in Table 1 based on the grey mathematical method. The samples are shown in Appendix A. The elastic parameters are assumed to obey normal distribution and the strength parameters are assumed to obey two-parameter Weibull distribution[52].

Table 1 The interval boundaries of elastic parameters and strength parameters

Elastic parameters	Lower bounds	Upper bounds	Strength parameters	Lower bounds	Upper bounds
$E_1\ (GPa)$	42.940	61.086	$X_t\ (MPa)$	465.247	531.420
$E_2\ (GPa)$	42.940	61.086	$X_c\ (MPa)$	121.144	157.178
$E_{12}\ (GPa)$	0.938	1.510	$Y_t\ (MPa)$	465.247	531.420
v_{12}	0.043	0.121	$Y_c\ (MPa)$	121.144	157.178
			$S_{12}\ (MPa)$	38.591	57.307

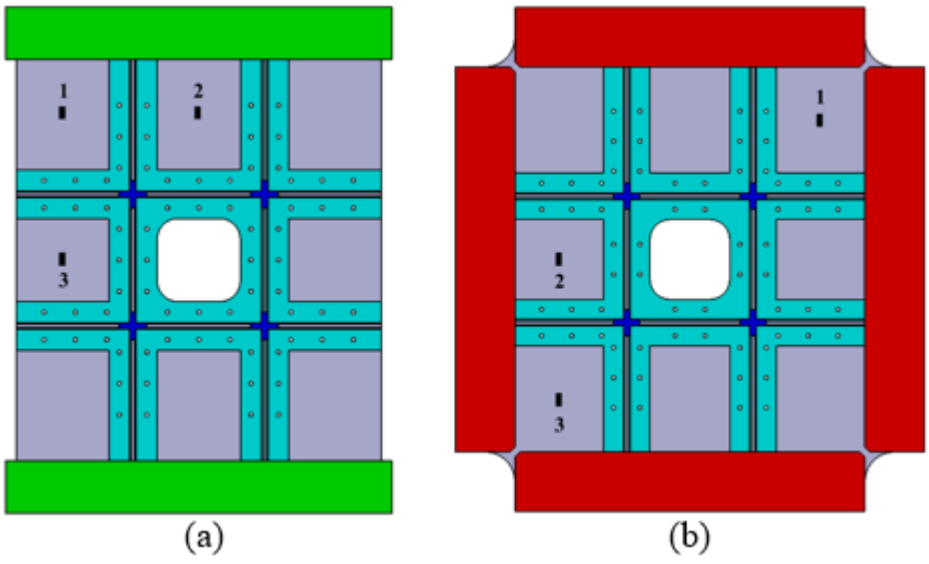

Figure 11 The strain measurement points of (a)CLC and (b)SLC

In FE model updating process, the structural responses include structural local strains, buckling loads and failure loads need to be considered. The reason for selecting these kind of respoonses are as follows. The structural local strains reflect the local elastic property, and the buckling loads reflect the global elastic property. The failure loads mirror the elastic and strength property of the FE model simultaneously. The ditribution diagram of the strain measurement points used for the model updating are shown in Figure 11. The compressive strains under the compressive load case and the in-plane shear strains under the shear load case are tested in the measurement points.

Before the model updating, the sensitivity analysis for the parameters of constraint condition (PoCCs) and uncertain parameters are performed to pick the sensitive parameters of constraint condition (PoCCs) and acertain the change regulation of the structural responses with the uncertain parameters vary. For the stiffened plate, the PoCCs for updating are the stiffness coefficients in different direction of the hinges and equivalent thickness of the fixture of the stiffened plate. The stiffness of hinges are picked out because the there inevitable exists gap in the hinges. The thickness of the fixture is chose since the space exists between the fixture and the specimen. The Latin hypercube design (LHD) is one of Design of experiments (DOE) methods with excellent abilities of space filling and nonlinear response fitting, and is utilized to carry on the sensitivity analysis. 1000 samples are adopted for the sensitivity analysis. The Pareto graph for structural responses are displayed in Figure 12. The lateral axis represent the factors affect the structural response. The factors include the elastic parameters, PoCCs and strength parameters. E_1, E_{12}, E_2, v_{12} are the elastic parameters; $k_1 \sim k_5$ and t is the PoCCs, namely, the stiffness of hinges and the equivalent thickness of the fixture, where $k_1 \sim k_3$ are the translational stiffness and $k_4 \sim k_5$ are the rotational stiffness (k_6 is defined as extremely small value); $X_t, X_c, Y_t, Y_c, S_{12}$ are the strength parameters. The longitudinal coordinates express the contribution rates for the structural responses induced by every factors. Different colors means different structural response influenced by the factors. $Strain\_1 \sim 3$ are the strains at different measurement points of the stiffened plate under shear load case. From the plots it can be seen that the PoCCs affect the elastic strains and failure load, where

$k_4 \sim k_5$ rarely affect the structural responses. At the same time, the elastic parameters have major infuence on the strains and failure load. Among the 5 strength parameters, the X_c is the most influential factor on the failure load. Thus the $k_1 \sim k_3$ and t are selected as the PoCCs to be updated.

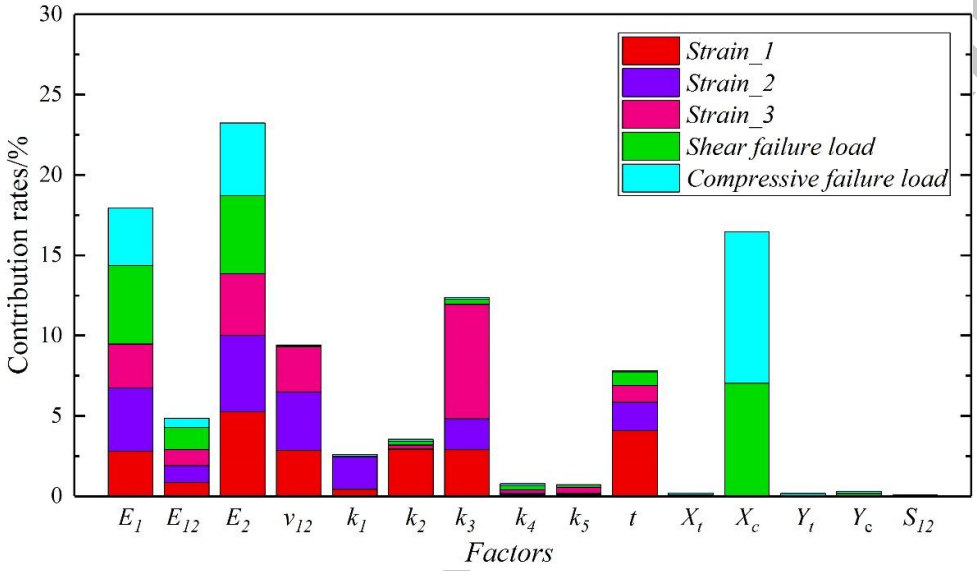

Figure 12 Pareto graph for structural response

Figure 13~Figure 15 show the effect trends of uncertainty parameters to strains, buckling load and Figure 13 shows that the structural strains and buckling load are monotonic with the uncertain variables. From Figure 14 and Figure 15 it can be seen that the failure loads are monotonic with the uncertain variables E_1, E_{12}, E_2, X_c. Although the rest uncertain variables have no monotonic relationship with the failure load, the contribution rates of them are little as shown in Figure 12 and can be neglected for the computational efficiency. Among the uncertainty propagation methods, the interval vertex method [53-55] can obtain the precise results when the maximum and minimum values fall on the interval vertexes. The amount of calculation is based on the number of the uncertain variables. The number of the structural analysis is 2^N (N is the number of uncertain variables). The interval bounds can be gained by the following equation

$$\overline{y} = \max_{i=1}^{2^N} \left\{ f\left(\boldsymbol{Z}_i, \boldsymbol{P}\right) \right\} \quad , \quad \underline{y} = \min_{i=1}^{2^N} \left\{ f\left(\boldsymbol{Z}_i, \boldsymbol{P}\right) \right\} \tag{21}$$

where $\boldsymbol{Z}$ is the interval parameter matrix, which can be expressed as

$$\boldsymbol{Z}=\begin{bmatrix} \underline{x}_1 & \underline{x}_2 & \cdots & \underline{x}_{N-1} & \underline{x}_N \\ \underline{x}_1 & \underline{x}_2 & \cdots & \underline{x}_{N-1} & \overline{x}_N \\ \vdots & \vdots & \ddots & \vdots & \vdots \\ \underline{x}_1 & \overline{x}_2 & \cdots & \overline{x}_{N-1} & \overline{x}_N \\ \overline{x}_1 & \overline{x}_2 & \cdots & \overline{x}_{N-1} & \overline{x}_N \end{bmatrix} \begin{matrix} 1 \\ 2 \\ \vdots \\ 2^N-1 \\ 2^N \end{matrix} \tag{22}$$

In this paper, the vertex method is applied for the solution of the uncertain intervals of the structural responses.

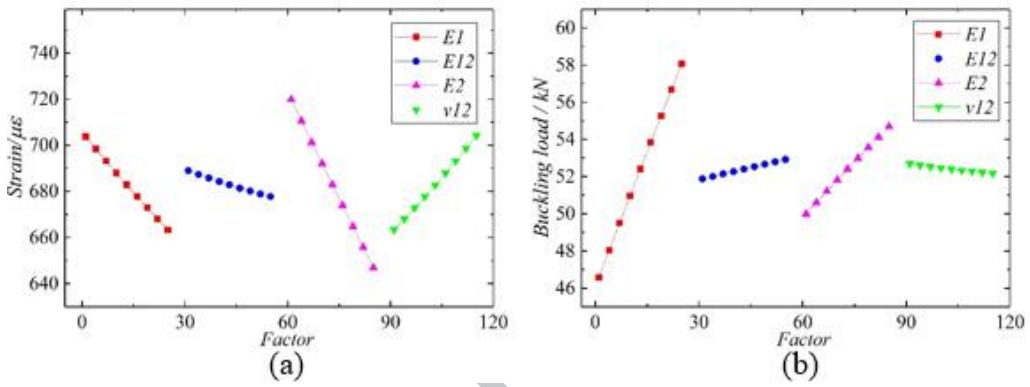

Figure 13 Effect trends of uncertainty parameters to (a) strains and (b) buckling load

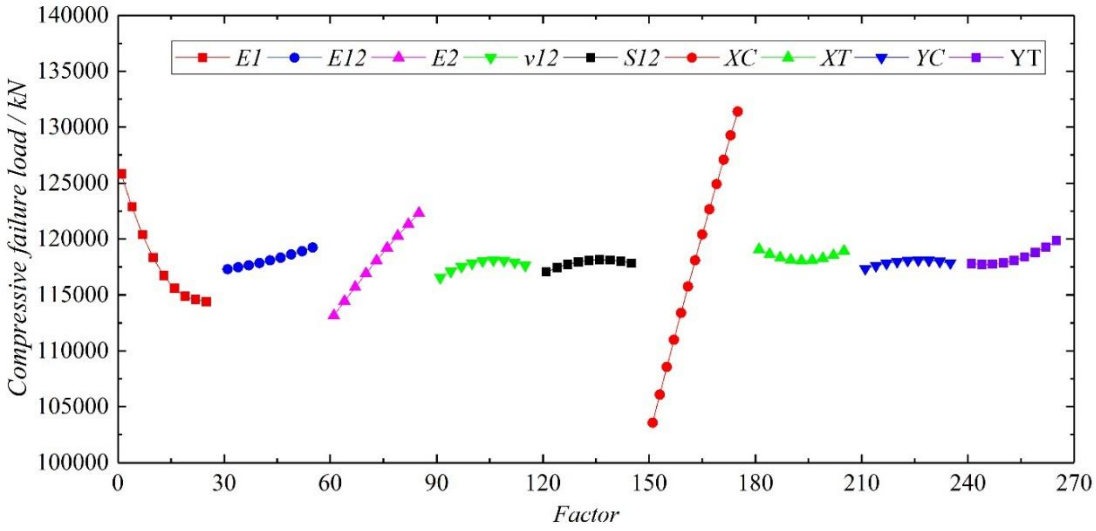

Figure 14 Effect trends of uncertainty parameters to compressive failure load

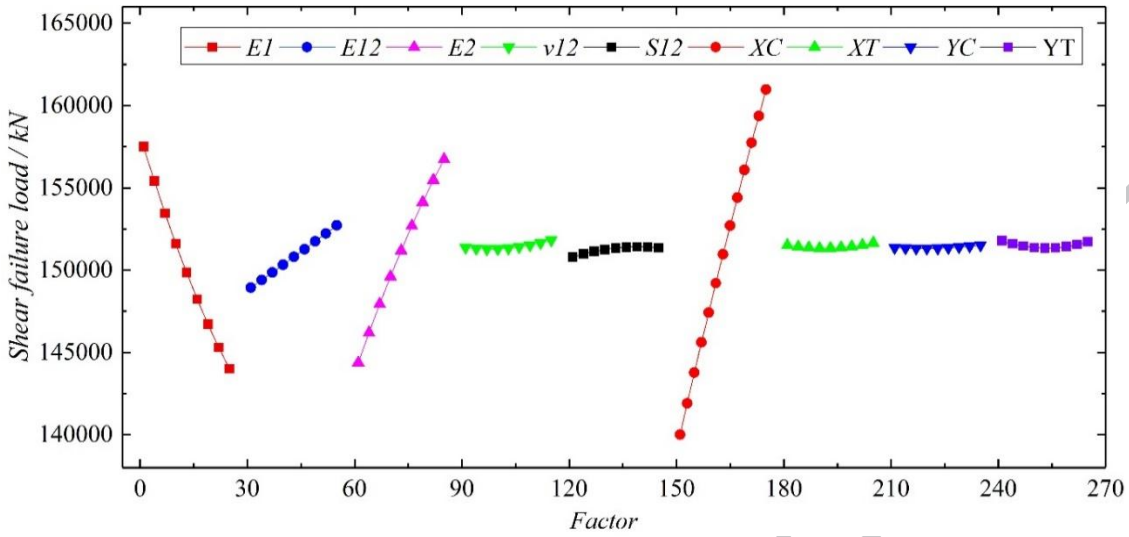

Figure 15 Effect trends of uncertainty parameters to shear failure load

The model updating was accomplished by the optimization method, which matches the responses of the FE model with the experimental datas, and the optimization model are as follows.

$$\begin{aligned} &\text{find} \quad k_i, t \qquad i = 1,2,3,4,5 \\ &\min \quad \sum_{j=1}^{q} w_j \frac{\left|\underline{y_j^{exp}} - \underline{y_j^{sim}\left(k_i, t, \boldsymbol{E}^I, \boldsymbol{X}^I\right)}\right| + \left|\overline{y_j^{exp}} - \overline{y_j^{sim}\left(k_i, t, \boldsymbol{E}^I, \boldsymbol{X}^I\right)}\right|}{0.5*\left(\overline{y_j^{\exp}} + \underline{y_j^{\exp}}\right)} \\ &\text{s.t.} \quad \boldsymbol{y} = \left\{y_j\right\} = \left[\boldsymbol{\varepsilon}, P, F\right] \end{aligned} \tag{23}$$

where k_i is the stiffness in different direction of the hinges; t is the equivalent thickness of the boundary of the stiffened plate; ε, P, F are the strain, buckling load, failure load, respectively; $\{w_j\}$ are the weighting coefficients of the responses, herein the values are all defined as unity; $\boldsymbol{E}^I, \boldsymbol{X}^I$ are the intervals of the elastic modulus and strength parameters, respectively. sim, exp represent the simulation and experimental values.

Through the model updating, the stiffness coefficients and the equivalent thickness of the fixture modified are shown as follows.

$$k_1 = 532546N/mm, k_2 = 180082N/mm, k_3 = 724937N/mm, t = 78.6mm \tag{24}$$

The simulated and experimental interval structural responses including the failure loads, the buckling loads and strains at different position are listed in Table 2. The experimental results are obtained based on the grey mathematics method and the sourse datas are listed in Appendix B. The

simulated intervals were calculated by the vertex method. It should be noted that the table only shows the compress buckling load, which is due to the shear failure load is less than the shear buckling load. In order to compare the difference between the experimental and the simulation results, the relative errors calculated by the middle values of experimental and numerical values are also listed in the table. The errors of the failure load, buckling load and strain are less than 5%, 2% and 7%, respectively. It can seen that the structural responses obtained from the FE models are almost tend to be consistent with the experimental results.

Table 2 the comparison between simulation and experimental value after model updating

	Load case		simulation	experiment	error
Failure load (kN)	compressive		$[96.7,139.9]$	$[99.8,127.2]$	4.2%
	shear		$[125.4,173.8]$	$[132.6,171.7]$	1.7%
Buckling load (kN)	compressive		$[39.7,64.0]$	$[44.4,60.6]$	1.2%
Strain ($\mu\varepsilon$)	compressive	1	$[347.1,625.4]$	$[399.5,515.6]$	6.3%
		2	$[242.8,395.4]$	$[279.1,375.9]$	2.6%
		3	$[314.7,578.2]$	$[375.7,483.8]$	3.9%
	shear	1	$[701.56,949.9]$	$[673.0,968.0]$	0.64%
		2	$[778.2,1091.7]$	$[792.6,1192.5]$	5.8%
		3	$[662.8,981.6]$	$[797.7,909.8]$	3.7%

The buckling modes and failure modes of the simulated results are compared with the experimental results to verify the rationality of the FE models. Herein, in order to simplify the coparison, the simulated results are displayed in which the uncertain parameters are defined as the middle values.

The experimental and simulated 1st buckling mode is shown in Figure 16 a) and Figure 16 b). Figure 16 a) shows the stiffened plate under the compressive load conditioin appeared large

displacement the middle of the panels, and second large displacement at the upper and lower parts of the panel. Figure 16 b) shows the simulated buckling mode, which is similar with the experimental phenomenon. The elastic property of the FE model is verified by the fact that the simulated buckling mode is in coincidence with the experimental result.

Figure 16 The 1st buckling mode: (a) experimental mode; (b) simulated mode

Figure 17 Failure patterns under (a) CLC and (b) SLC

Figure 17 (a) and Figure 17(b) show the failure patterns of the stiffened plate under compressive load and shear load. Figure 18 shows the simulated damage evolution process of the stiffened plate under the compressive load case. The elements which are in longitudinal compression failure mode in the 0^o layer are marked in red. The failure mechanism of the stiffened plate under compressive load case is that the large deformation occurred in the intermediate position of panel lead to the flexural fracture after instability, then the fracture extend to the free end from the openning position, which lead to the total failure of the structure. The failure pattern of the experimental and simulated stiffened plate extent the same at the start point of the failure. It is important to note that the fracture path of the experimental stiffened plate arise in the one side of the panel, however the symetric failure mode arise in the simulated stiffened plate. The difference is

come from the initial defect of the experimental samples is always asymmetrical, which lead to the one-side failure path.

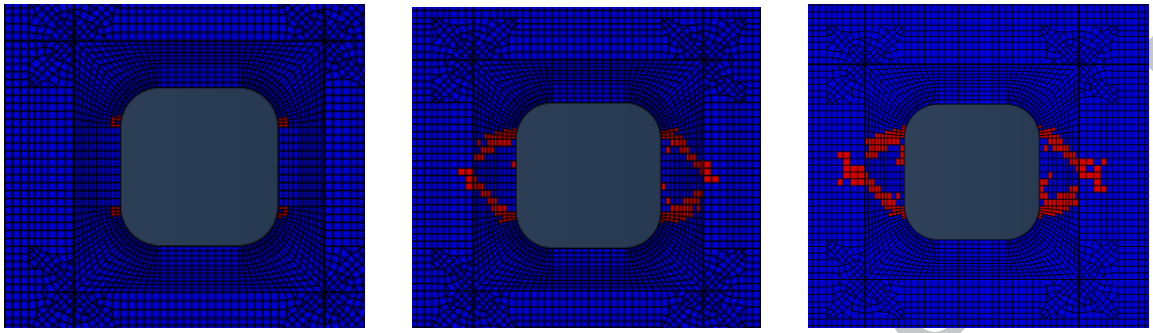

a) 76.5% $F_{failure}$ b) 95% $F_{failure}$ c)100% $F_{failure}$

Figure 18 The damage evolution process under the compressive load case

Figure 19 shows the simulated damage evolution process under the shear load case. The elements which are in longitudinal compression failure mode in the 45^{o} layer are signed in red. The failure mechanism of the stiffened plate under shear load case is that the compression damage appears at the compression corner, then the failure path extends along the diagonal direction of the panel until the stiffened plate lose its capacity. The experiment and simulation for the damage evolution perform alike at the beginning position of the failure. The comparisions between the experiments and simulations indicate that the FE models have enough accuracy in the characterization for the strength property of real structures.The strength property of the FE model is verified by the fact that the simulated failure mode is in coincidence with the experimental result.

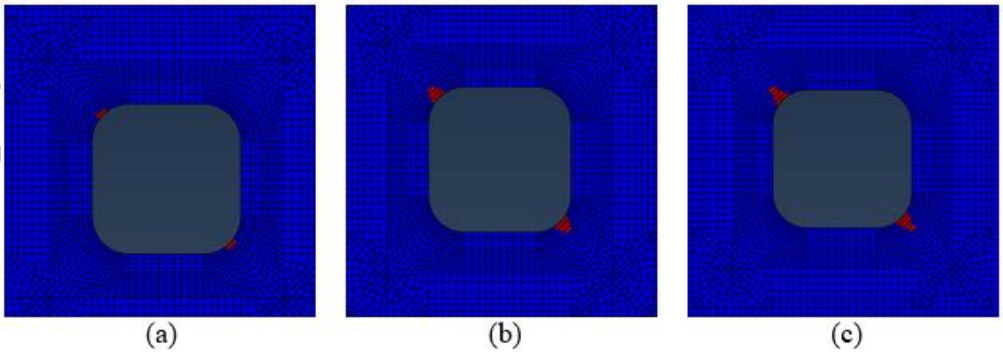

Figure 19 The damage evolution under the SLC: (a) 73% $F_{failure}$; (b) 85% $F_{failure}$; (c)100% $F_{failure}$

Above of all, the local and whole elastic property of the FE model are verified by the strains and buckling load and mode. The strengh property of the FE model is proved through the failure

load and failure mode. Thus, the constructed FE model can be utilized to process the following optimization procedure.

5.2. The SF based optimization for the laminate

After updating the FE model, the SF based optimization method is utilized to optimize the stiffened plate. The candidate ply orientations are selected as 0^o and 45^o, which is due to the following reasons. On the one hand, the layers of 0^o is usually utilized to bear the in-plane compressive loads; the layers of 45^o is usually utilized to bear the shear load. On the other hand, in the process of design and manufacture, the the number of laying directions should be minimized in order to simplify the workload. The elastic parameters are defined as the middle values, and the strength parameters are defined as the lower bounds of their intervals. The optimization model is as follows.

$$\begin{aligned} &\min \quad W \\ &\text{find} \quad n_0, n_{45} \\ &\text{s.t.} \quad F_{shear} \geq n_{shear} \times \left[F_{shear} \right], F_{compress} \geq n_{compress} \times \left[F_{compress} \right] \end{aligned} \tag{25}$$

where W is the mass of the composite stiffened plate; n_0, n_{45} are the numbers of 0^o and 45^o plies in the structure, which is preparation for the second-step optimization; $F_{shear}, F_{compress}$, are the failure loads in shear and compress load cases; $\left[F_{shear} \right], \left[F_{compressive} \right]$ are the critical failure load in shear and compressive load cases. $n_{shear}, n_{compress}$ are the SFs in shear and compressive load cases. Herein, $n_{shear} = n_{compress} = 1.1$, which is defined as the same effects caused by the uncertainty of elastic modular parameters. $\left[F_{shear} \right]$, $\left[F_{compress} \right]$ are the allowable load, and $\left[F_{shear} \right]$=112.0kN, $\left[F_{compress} \right]$=89.1kN.

Table 3 the number of plies and weight of the initial and SF based design scheme

Component	Panels		Ribs		Reinforced piece, cap ridge		Weight
Stacking angle	0°	45°	0°	45°	0°	45°	(kg)
Initial design scheme	6	5	6	5	6	5	1.295
SF based design scheme	6	5	6	3	6	5	1.251

The Hooke and Jeeves (HJ) algorithm[56] is utilized to solve the optimization model, where the initial point is the initial layer scheme, corresponding to the intact state of the structure. The relative step size is 0.02 and step size reduction factor is 0.5. Through the first-level super-layer thickness optimization, the optimized number of plies of different components are shown in Table 3. The structural weight of composite stiffened plate can be reduced up to 3.5%. Then the stacking sequence library is established and the stacking sequence optimization of the composite stiffened plate is executed with global algorithm in the second level. The SF based second-level optimization model is expressed as

$$\begin{aligned} &\max \quad F_{shear}, F_{compress} \\ &\text{find} \quad \{\theta_u\}, (u = 0^o, 45^o) \\ &\text{s.t.} \quad g_{j^*}(t) \le 0, \quad j^* = 1, 2, \ldots \\ &\qquad F_{shear} \ge n \times \left[F_{shear}\right], F_{compress} \ge n \times \left[F_{compress}\right] \end{aligned} \tag{26}$$

where $\{\theta_u\}$ is the stacking sequence libraries of different components. The candidate angles are $0^o, 45^o$ for the woven materials. $g_{j^*}(t) \le 0$ is the manufacturing constraints.

Table 4 The stacking sequence scheme based on the SF method

Component	Stacking sequence
Panels	$[45^o / 0_2^o / 45^o / 0^o / \overline{45^o}]_s$
Ribs	$[0_2^o / 45^o / 0^o / \overline{45^o}]_s$
Reinforced piece, cap ridge	$[45^o / 0_2^o / 45^o / 0^o / \overline{45^o}]_s$

The genetic algorithm [57] is utilized to solve the optimization model. The final stacking sequence scheme based on the SF method for composites is shown in Table 4. From the table one can see that the stacking sequence scheme based on the SF method is different from the initial stacking sequence scheme. The failure loads of the initial scheme and two-step optimization results are shown in Table 5. The table shows that through the two-step optization process, the compression failure load is not improved and the shear failure load is improved. The reason may be that the

secongd top 45^o layers of the panels in the initial scheme are transferred to the top layer, which reduced the compression capacity and improved the shear capacity. Nevertheless, the designed scheme still satisfies the requirement of the critical load.

Table 5 the failure load of the SF based optimization result

	Compression failure load	Shear failure load
Initial scheme	99.6 kN	128.2 kN
thickness optimization	98.5 kN	128.2 kN
stacking sequence optimization	98.5 kN	128.4 kN

5.3. The NPR based optimization for the laminate

In this part, the optimization based on NPR theory is performed and the optimization scheme is verified experimentally. Before the optimization, the NPR of the SF based optimization scheme is calculated for the constraint condition. The uncertainty analysis is performed based on the uncertain parameters including the elastic and strength parameters. The interval bounds of the failure load are calculated and the non-probabilistic index is obtained. The interval bounds of the compressive failure load are $\left[93.4\text{kN},136.2\text{kN}\right]$, and the interval bounds of shear failure load are $\left[111.5\text{kN},153.6\text{kN}\right]$. The corresponding non-reliabilities are $\left[R_{SF}^{compress}\right]=100\%$ and $\left[R_{SF}^{shear}\right]=98.8\%$, respectively. Similar to the optimization method based on SF, the NPR based optimization is performed in two stages as the thickness optimization and stacking sequence optimization. The optimization model is shown in(27), where $\boldsymbol{E}^I, \boldsymbol{X}^I$ represent $\boldsymbol{x}^{\mathrm{I}}$ in Eq.(4) and $[F_{shear}^I; F_{compress}^I]$ express $\boldsymbol{y}^I$ in Eq.(4). The HJ algorithm is used for the thickness optimization, and the optimization results are shown in Table 6. The table shows that the number of the stiffened plate is reduced compared with the SF based design scheme, and the reduced ratio of weight is up to 7.6%.

$$\begin{aligned} &\min \quad W \\ &\text{find} \quad n_0, n_{45} \\ &\text{s.t.} \quad R\left(F_{shear}^I\left(\boldsymbol{E}^I, \boldsymbol{X}^I\right)-\left[F_{shear}\right]\right)\geq\left[R_{SF}^{shear}\right] \\ &\qquad R\left(F_{compress}^I\left(\boldsymbol{E}^I, \boldsymbol{X}^I\right)-\left[F_{compress}\right]\right)\geq\left[R_{SF}^{compress}\right] \end{aligned} \tag{27}$$

Table 6 The number of plies and weight of the SF and NPR based design scheme

Component	Panels		Ribs		Reinforced piece, cap ridge		Weight
Stacking angle	0°	45°	0°	45°	0°	45°	(kg)
SF based design scheme	6	5	6	3	6	5	1.251
NPR based design scheme	6	5	6	3	6	3	1.156

Next, the sequence stacking optimization utilizing the genetic algorithm is processed based on the optimization model shown in Eq.(28). The stacking sequence scheme optimized in shown in Table 7. Through the FE analysis and uncertainty analysis, the interval of the failure load is obtained. The interval bounds of the compressive failure load are $\left[91.7\text{kN},131.9\text{kN}\right]$, and the shear failure load is $\left[112.4\text{kN},157.1\text{kN}\right]$. The corresponding non-reliabilities are both 100% in the two load cases.

$$\begin{aligned} &\max \quad \underline{F_{shear}},\underline{F_{compress}} \\ &\text{find} \quad \{\theta_u\},(u=0^o,45^o) \\ &\text{s.t.} \quad R\left(F^I_{shear}\left(X^I,E^I\right)-\left[F_{shear}\right]\right)\geq\left[R^{shear}_{SF}\right] \\ &\qquad R\left(F^I_{compress}\left(X^I,E^I\right)-\left[F_{compress}\right]\right)\geq\left[R^{compress}_{SF}\right] \end{aligned} \tag{28}$$

Table 7 The stacking sequence scheme based on the NPR method

Component	Stacking sequence
Panels	$[0^o/45^o_2/0^o_2/\overline{45^o}]_s$
Ribs	$[0^o/45^o/0^o_2/\overline{45^o}]_s$
Reinforced piece, cap ridge	$[0^o/45^o/0^o_2/\overline{45^o}]_s$

In order to verify the validity of optimization result, the specimens for the shear load and compressive load based on the stacking sequence in Table 7 were manufactured and the destructive tests were carried out. The load-displacement curves of the stiffened plate under the two load cases are shown in Figure 20, which display the failure load as the load drop point. For the convenience of comparison and analysis, the test results and simulated results are together listed in Table 8. From

the table one can see that the experimental failure loads have fallen in the simulated intervals of the failure load, which proved the effectiveness of the built FE model. The reliabilities of the NPR based method are improved compared with the reliabilities of the SF based method. That is owing to the nominal values and radii of failure load were both optimization variables and the intervals were narrowed. Thus the reliability based method can be reckoned as superior to the SF based method when the intervals can be narrowed. It should be noted that the interval of the responses cannot always be reduced.

Table 8 the simulated reslut and test reslut of bearing capacity

Load case	Critical load (kN)	The interval of failure load (kN)		Experimental (kN)
		SF based	Reliability based	
compress	89.1	[93.4,136.2]	[91.7,131.9]	104.9
shear	110.0	[111.5,153.6]	[112.4,152.1]	126.8

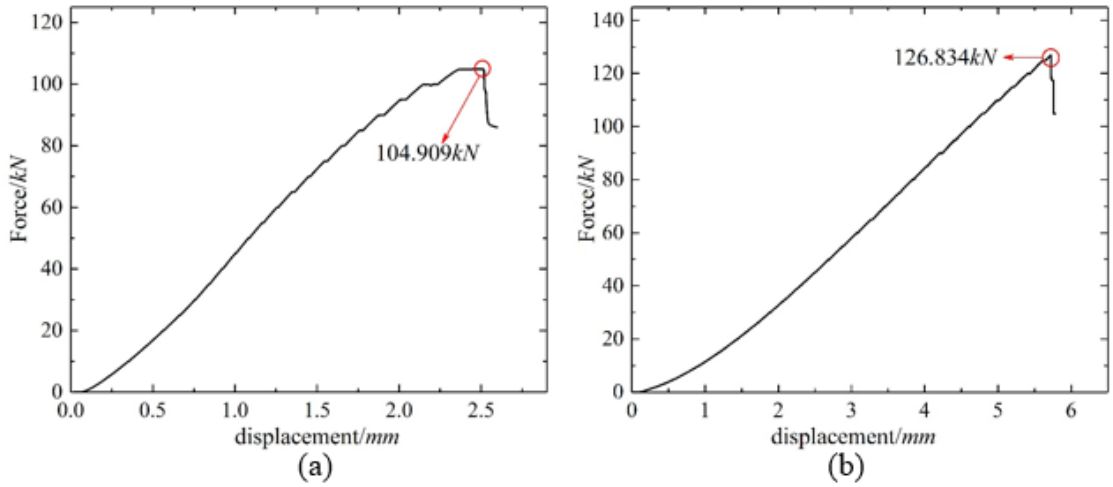

Figure 20 Load-displacement curves of the stiffened plate: (a)CLC; (b)SLC.

6. Conclusion

This paper proposes an interval model updating based uncertain optimization for the composite structures. The interval model updating method is performed to determine the boundary condition, through which the simulated interval bounds of the responses will coincide with the experimental ones. A new uncertain optimization method for composite structures based on progressive failure

theory, which overcomes the limitation of FPF and LPF for the failure analysis and SF based method for the uncertainty analysis. The reliability constraint for the NPR based method is defined as the of the NPR of the optimization scheme based on SF method. The proposed method was verified by an experimental work of the stiffened plate under two load cases. The FE model was updated under uncertainty conditions based on the proposed interval model updating theory. The structural responses including local strains, buckling loads and failure loads were close to the real measurements in the experiments by updating the constraint parameters. The SF based optimization and NPR based optimization were carried out one after another. The weight of the SF based optimization scheme was reduced under the constraint of the allowable failure load. The NPR based optimization was performed to increase the reliability of the composite stiffened plate. The reliabilities were increased and the weight is reduced by the reliability based method compared with the SF based method, which proved the superiority of the reliability based method to the SF based method when the intervals of the structural responses can be narrowed by optimization. The optimal composite stiffened plates under different load cases based on the reliability theory were fabricated and the failure loads were tested, and the failure load fell in the interval estimation, which proved the validity of the proposed method.

Acknowledgement

This work is supported by the National Key Research and Development Program (2016YFB0200700), the National Nature Science Foundation of the P.R. China (11872089, 11432002 and 11572024), the Defence Industrial Technology Development Program (JCKY2016204B101, JCKY2016601B001), and the 111 Project (B07009) for the financial supports.

Appendix A. The samples of material parameters

No.	1	2	3	4	5	6	7	8	9	10
$E_1\ (GPa)$	57.95	48.86	49.34	55.08	51.64	49.23	49.92	49.17	57.08	51.87
$E_{12}\ (GPa)$	1.22	1.41	1.19	1.05	1.21	1.08	1.35	1.33	1.15	1.25
$E_2\ (GPa)$	57.95	48.86	49.34	55.08	51.64	49.23	49.92	49.17	57.08	51.87
v_{12}	0.064	0.053	0.075	0.058	0.065	0.072	0.055	0.058	0.065	0.071
$X_t\ (MPa)$	516.20	498.56	479.10	516.39	489.93	521.51	519.56	516.21	522.51	505.58
$X_c\ (MPa)$	142.93	133.09	154.85	145.33	151.65	141.47	147.09	144.85	137.33	149.23
$Y_t\ (MPa)$	516.20	498.56	479.10	516.39	489.93	521.51	519.56	516.21	522.51	505.58
$Y_c\ (MPa)$	142.93	133.09	154.85	145.33	151.65	141.47	147.09	144.85	137.33	149.23
$S_{12}\ (MPa)$	49.12	54.92	47.00	49.64	51.52	46.72	55.40	46.36	53.68	51.76

Appendix B. The samples of material parameters

No.			1	2	3	4
Failure load (kN)	Compressive		114.1	114.8	120.2	105.8
	Shear		154.6	140.5	159.5	155.2
Buckling load (kN)	Compressive		50	55	55	50
Strain ($\mu\varepsilon$)	Compressive	1	476	436	443	475
		2	353	332	310	315
		3	419	407	459	434
	Shear	1	912	817	800	753
		2	924	937	1049	1060
		3	854	819	873	869

Reference

[1] Xia Q, Shi T L. A cascadic multilevel optimization algorithm for the design of composite structures with curvilinear fiber based on Shepard interpolation [J]. Composite Structures, 2018, 188: 209-219.

[2] Rao A R M, Lakshmi K. Multi-objective Optimal Design of Hybrid Laminate Composite Structures Using Scatter Search [J]. Journal of Composite Materials, 2009, 43(20): 2157-2182.

[3] Lopez R H, Miguel L F F, Belo I M, Cursi J E S. Advantages of employing a full characterization method over FORM in the reliability analysis of laminated composite plates [J]. Composite Structures, 2014, 107: 635-642.

[4] Zhou X Y, Gosling P D, Ullah Z, Kaczmarczyk L, Pearce C J. Exploiting the benefits of multi-scale analysis in reliability analysis for composite structures [J]. Composite Structures, 2016, 155: 197-212.

[5] Qian C, Shi W, Chen Z, Yang S, Song Q. Fatigue reliability design of composite leaf springs based on ply scheme optimization [J]. Composite Structures, 2017, 168: 40-46.

[6] Schillo C, Kriegesmann B, Krause D. Reliability based calibration of safety factors for unstiffened cylindrical composite shells [J]. Composite Structures, 2017, 168: 798-812.

[7] Aslani F, Lloyd R, Uy B, Kang W H, Hicks S. Statistical calibration of safety factors for flexural stiffness of composite columns [J]. Steel & Composite Structures, 2016, 20(1): 127-145.

[8] The stochastic finite element method:basic perturbation technique and computer implementation [M]. Wiley.

[9] Wang L, Cai Y R, Liu D L. Multiscale reliability-based topology optimization methodology for truss-like microstructures with unknown-but-bounded uncertainties [J]. Computer Methods in Applied Mechanics and Engineering, 2018, 339: 358-388.

[10] Wang L, Liang J X, Yang Y W, Zheng Y N. Time-dependent reliability assessment of fatigue crack growth modeling based on perturbation series expansions and interval mathematics [J]. Theoretical and Applied Fracture Mechanics, 2018, 95: 104-118.

[11] Wang L, Xiong C, Yang Y W. A novel methodology of reliability-based multidisciplinary design optimization under hybrid interval and fuzzy uncertainties [J]. Computer Methods in Applied Mechanics and Engineering, 2018, 337: 439-457.

[12] Cederbaum G, Elishakoff I, Librescu L. Reliability of laminated plates via the first-order second-moment method [J]. Composite Structures, 1990, 15(2): 161-167.

[13] Rackwitz R, Flessler B. Structural reliability under combined random load sequences [J]. Computers & Structures, 1978, 9(5): 489-494.

[14] Sobey A J, Blake J I R, Shenoi R A. Monte Carlo reliability analysis of tophat stiffened composite plate structures under out of plane loading [J]. Reliability Engineering & System Safety, 2013, 110(2): 41-49.

[15] Stefanou G. The stochastic finite element method: Past, present and future [J]. Computer Methods in Applied Mechanics & Engineering, 2009, 198(9–12): 1031-1051.

[16] Patel S, Guedes Soares C. Reliability assessment of glass epoxy composite plates due to low velocity impact [J]. Composite Structures, 2018, 200: 659-668.

[17]Wang X J, Qiu Z, Elishakoff I. Non-probabilistic set-theoretic model for structural safety measure [J]. Acta Mechanica, 2008, 198(1-2): 51-64.
[18]Kang Z, Luo Y J. Reliability-based structural optimization with probability and convex set hybrid models [J]. Structural & Multidisciplinary Optimization, 2010, 42(1): 89-102.
[19]Simoen E, Roeck G D, Lombaert G. Dealing with uncertainty in model updating for damage assessment: A review [J]. Mechanical Systems & Signal Processing, 2015, 56-57(56): 123-149.
[20]Titurus B, Friswell M I. Regularization in model updating [J]. International Journal for Numerical Methods in Engineering, 2008, 75(4): 440-478.
[21]VanDerHorn E, Mahadevan S. Bayesian model updating with summarized statistical and reliability data [J]. Reliability Engineering & System Safety, 2018, 172: 12-24.
[22]Su T-L, Jaki T, Hickey G L, Buchan I, Sperrin M. A review of statistical updating methods for clinical prediction models [J]. Statistical Methods in Medical Research, 2018, 27(1): 185-197.
[23]Möller B, Beer M. Engineering computation under uncertainty – Capabilities of non-traditional models [J]. Computers & Structures, 2008, 86(10): 1024-1041.
[24]Khodaparast H H, Mottershead J E, Badcock K J. Interval model updating with irreducible uncertainty using the Kriging predictor [J]. Mechanical Systems & Signal Processing, 2011, 25(4): 1204-1226.
[25]Fang S E, Zhang Q H, Ren W X. An interval model updating strategy using interval response surface models [J]. Mechanical Systems and Signal Processing, 2015, 60-61: 909-927.
[26]Jiang C, Long X Y, Han X, Tao Y R, Liu J. Probability-interval hybrid reliability analysis for cracked structures existing epistemic uncertainty [J]. Engineering Fracture Mechanics, 2013, 112: 148-164.
[27]Kang Z, Luo Y. Reliability-based structural optimization with probability and convex set hybrid models [J]. Structural and Multidisciplinary Optimization, 2010, 42(1): 89-102.
[28]Luo Y, Wu X, Zhou M, Wang M Y. Simultaneous parameter and tolerance optimization of structures via probability-interval mixed reliability model [J]. Structural and Multidisciplinary Optimization, 2015, 51(3): 705-719.
[29]Wang L, Wang X, Xia Y. Hybrid reliability analysis of structures with multi-source uncertainties [J]. Acta Mechanica, 2014, 225(2): 413-430.
[30]Zhao J, Fan X, Sun Q. Stacking sequence optimization of composite laminates for maximum buckling load using permutation search algorithm [J]. Composite Structures, 2015, 121(121): 225-236.
[31]Meng Z, Hao P, Li G, Wang B, Zhang K. Non-probabilistic reliability-based design optimization of stiffened shells under buckling constraint [J]. Thin-Walled Structures, 2015, 94: 325-333.
[32]de Almeida F S. Stacking sequence optimization for maximum buckling load of composite plates using harmony search algorithm [J]. Composite Structures, 2016, 143: 287-299.
[33]Chen X, Wang X J, Qiu Z P, Wang L, Li X, Shi Q H. A novel reliability-based two-level optimization method for composite laminated structures [J]. Composite Structures, 2018, 192: 336-346.
[34]Jing Z, Fan X, Sun Q. Global shared-layer blending method for stacking sequence optimization design and blending of composite structures [J]. Composites Part B-Engineering, 2015, 69:

181-190.
[35] Tannor D. Introduction to quantum mechanics [M]. Sausalito: University Science Books, 2007.
[36] Biegler L, Biros G, Ghattas O, Heinkenschloss M, Keyes D, Mallick B, Tenorio L, van Bloemen Waanders B, Willcox K, Marzouk Y. Large-scale inverse problems and quantification of uncertainty [M]. New Jersey: John Wiley & Sons, 2011.
[37] Grigoriu M. Stochastic systems: uncertainty quantification and propagation [M]. New York: Springer Science & Business Media, 2012.
[38] Wang X J, Wang L, Qiu Z P. A feasible implementation procedure for interval analysis method from measurement data [J]. Applied Mathematical Modelling, 2014, 38(9-10): 2377-2397.
[39] Chen X, Wang X, Wang L, Shi Q, Li Y. Uncertainty quantification of multi-dimensional parameters for composite laminates based on grey mathematical theory [J]. Applied Mathematical Modelling, 2018, 55: 299-313.
[40] Soize C. Generalized probabilistic approach of uncertainties in computational dynamics using random matrices and polynomial chaos decompositions [J]. International Journal for Numerical Methods in Engineering, 2010, 81(8): 939-970.
[41] Hashin Z. Failure Criteria for Unidirectional Fiber Composites [J]. Journal of Applied Mechanics, 1980, 47(2): 329-334.
[42] A.Puck, H.Schurmann. Failure Analysis of FRP Laminates [J]. 1998.
[43] Chang F K, Chang K Y. A Progressive Damage Model for Laminated Composites Containing Stress Concentrations [J]. Journal of Composite Materials, 1987, 21(9): 834-855.
[44] Pinho S T, Davilla C G, Camanho P P, Iannucci L, Robinson P. Failure Models and Criteria for FRP Under In-Plane or Three-Dimensional Stress States Including Shear Non-Linearity [J]. Nasa Technical Memorandum, 2005.
[45] Luo H B, Yan Y, Meng X J, Jin C. Progressive failure analysis and energy-absorbing experiment of composite tubes under axial dynamic impact [J]. Composites Part B, 2016, 87: 1-11.
[46] Chang F K, Scott R A, Springer G S. Strength of Mechanically Fastened Composite Joints [J]. Journal of Composite Materials, 1982, 16(6): 470-494.
[47] Pisano A A, Fuschi P. Mechanically fastened joints in composite laminates: Evaluation of load bearing capacity [J]. Composites Part B Engineering, 2011, 42(4): 949-961.
[48] Wang L, Liu D L, Yang Y W, Wang X J, Qiu Z P. A novel method of non-probabilistic reliability-based topology optimization corresponding to continuum structures with unknown but bounded uncertainties [J]. Computer Methods in Applied Mechanics and Engineering, 2017, 326: 573-595.
[49] Li Q, Qiu Z P, Zhang X D. Eigenvalue analysis of structures with interval parameters using the second-order Taylor series expansion and the DCA for QB [J]. Acta Mechanica Sinica, 2015, 31(6): 845-854.
[50] Xu M H, Du J K, Wang C, Li Y L. A dimension-wise analysis method for the structural-acoustic system with interval parameters [J]. Journal of Sound & Vibration, 2017, 394: 418-433.
[51] Wang X J, Wang L, Qiu Z P. Safety estimation of structural systems via interval analysis [J]. Chinese Journal of Aeronautics, 2013, 26(3): 614-623.
[52] Sriramula S, Chryssanthopoulos M K. Quantification of uncertainty modelling in stochastic

analysis of FRP composites [J]. Composites Part a-Applied Science and Manufacturing, 2009, 40(11): 1673-1684.
[53] Qiu Z P, Lv Z. The vertex solution theorem and its coupled framework for static analysis of structures with interval parameters [J]. International Journal for Numerical Methods in Engineering, 2017, 112(7): 711-736.
[54] Qiu Z P, Wang X J, Friswell M I. Eigenvalue bounds of structures with uncertain-but-bounded parameters [J]. Journal of Sound and Vibration, 2005, 282(1-2): 297-312.
[55] Qiu Z P, Xia Y Y, Yang J L. The static displacement and the stress analysis of structures with bounded uncertainties using the vertex solution theorem [J]. Computer Methods in Applied Mechanics & Engineering, 2007, 196(49): 4965-4984.
[56] Rios-Coelho A C, Sacco W F, Henderson N. A Metropolis algorithm combined with Hooke–Jeeves local search method applied to global optimization [J]. Applied Mathematics & Computation, 2010, 217(2): 843-853.
[57] Herath M T, Prusty B G, Phillips A W, St. John N. Structural strength and laminate optimization of self-twisting composite hydrofoils using a Genetic Algorithm [J]. Composite Structures, 2017, 176: 359-378.